Specific Contribution of Neurons From the Dbx1 Lineage to The Piriform Cortex

Thando Shabangu
Academia Sinica
Hung-Lun Chen
Graduate Institute of Life Sciences, National Defense Medical Center
Zi-hui Zhuang
Academia Sinica
Alessandra Pierani
Université de Paris, Imagine Institute
Chien-Fu Chen
Graduate Institute of Life Sciences, National Defense Medical Center
Shen-Ju Chou (schou@gate.sinica.edu.tw)
Academia Sinica

Research Article

Keywords: piriform cortex, MOB, olfactory cortex

Posted Date: December 17th, 2020

DOI: https://doi.org/10.21203/rs.3.rs-126014/v1

Version of Record: A version of this preprint was published at Scientific Reports on April 16th, 2021. See the published version at https://doi.org/10.1038/s41598-021-86512-8.

Specific contribution of neurons from the Dbx1 lineage to the piriform cortex

Thando Shabangu[1, 2, 3], Hung-Lun Chen[2], Zi-hui Zhuang[1], Alessandra Pierani[4,5], Chien-Fu F. Chen[2,3,*], and Shen-Ju Chou[1,3,*]

1. Institute of Cellular and Organismic Biology, Academia Sinica, Taipei, Taiwan

2. Graduate Institute of Life Sciences, National Defense Medical Center, Taipei, Taiwan

3. Molecular Cell Biology, Taiwan International Graduate Program, Academia Sinica, Taipei, Taiwan

4. Université de Paris, *Imagine* Institute, Team Genetics and Development of the Cerebral Cortex, F-75015, Paris, France

5. Université de Paris, Institute of Psychiatry and Neuroscience of Paris, INSERM U1266, F-75014, Paris, France

*Corresponding authors:

Shen-Ju Chou

Institute of Cellular and Organismic Biology, Academia Sinica,

128 Academia Rd. Sec. 2, Taipei, 11529, Taiwan.

Tel: 886-2-2789-9530

Email: schou@gate.sinica.edu.tw

Chien-Fu F. Chen

Graduate Institute of Life Sciences, National Defense Medical Center,

No.161, Sec. 6, Minquan E. Rd., Taipei,114, Taiwan

Tel: 886-2-8792-3100 ext:18572

Email: t70cyy@yahoo.com

Abstract

The piriform cortex (PC) is a major cortical processing center for the sense of smell that receives direct inputs from the olfactory bulb. In mice, the PC consists of three neuronal layers, which are populated by cells with distinct developmental origins. One of developmental origins of PC is the Dbx1-expressing neural progenitors located in the ventral pallium at the pallial-subpallial boundary. Since the precise mechanisms of PC neuron development are largely unknown, we sought to define the distribution, timing of neurogenesis, morphology and projection patterns of PC neurons from the Dbx1 lineage. We found that Dbx1-lineage neurons are preferentially distributed in layer 2 and enriched in the ventral portion of the PC. Further, Dbx1 neurons are early-born neurons that contribute to most neuronal subtypes in the PC. Our data also revealed an enrichment of Dbx1-lineage neurons located in the ventral anterior PC that project to the orbitofrontal cortex. These findings suggest a specific association between developmental origin of PC neurons and their neuronal properties.

Introduction

Odors are potent signals that can convey information through time and space [1]. To process these signals, most mammals rely on the olfactory system, a three-level neural pathway that comprises a sensor sheet (the olfactory epithelium; OE), a primary processing level (main olfactory bulb; MOB), and a secondary processing level (the olfactory cortex). The connections between sensory neurons of the OE and principal neurons of the MOB follow wiring principles that depend on sensory neuron receptor choice. Thus, a stereotypic afferent organization is found in the MOB [2], which can explain topographic odor representation at the primary processing level. Beyond the MOB, odor information is dispatched via axons of the principal neurons, mitral and tufted cells, to several paleo- and neocortical areas that are together termed the olfactory cortex (OC). The projections of mitral and tufted cells to the OC are highly distributed [3,4], leading to highly distributed odor representation in most OC areas [5-8]. While the overall organization of the olfactory system is known, how the OC contributes to odor perception is still an open question.

Piriform cortex (PC) is the largest area in the OC and it receives a complete set of MOB projections [3]. The PC is divided into two anatomically and functionally distinct sub-regions, the anterior PC (APC) and posterior PC (PPC) [9,10]. Additionally, based on cytoarchitecture and connectivity, the APC can be further divided into dorsal and ventral subdomains. These distinct PC subregions have different input and output projection patterns (Illig, 2005; Mazo et al., 2017; Murphy and Deutch, 2018). For example, the ventral APC receives inputs from both mitral and tufted cells in the olfactory bulb, while dorsal APC and PPC only receive inputs from the mitral cells [9,11,12]. Furthermore, the projection neurons in the ventral APC predominantly project to the lateral orbital cortex [9,13]. Based on these specific inputs and outputs, the PC sub-regions likely contribute differently to olfactory processing.

Cortical columns in the PC consist of three neuronal layers. The outermost layer is called layer 1 (L1); it is a superficial plexiform layer, containing axons of mitral and tufted cells mostly within L1a and association fibers from other PC and

cortical areas in L1b [14]. Layer 2 (L2) is the most cell-dense layer in the PC, and it is further subdivided into an outer layer 2a (L2a) and inner layer 2b (L2b). L2a is predominately occupied by semilunar cells, while L2b consists mainly of pyramidal neurons. Compared to L2, layer 3 (L3) has a relatively low density of neurons, most of which are large pyramidal neurons. In contrast to the six-layer neocortex, the developmental process of the three-layer piriform cortex remains poorly understood, at least partially due to the fact that PC neurons originate from multiple sources, including both the lateral and ventral pallium [15-17].

In this study, we sought to define the contribution of a specific lineage, the Dbx1 (developing brain homeobox 1) lineage, in the PC. Dbx1 is a homeodomain transcription factor involved in neuronal fate specification [18-20]. During early corticogenesis, Dbx1 is highly expressed in the preoptic area (POA), in the septum and ventral pallium (VP) at the pallial-subpallial border (PSB) in the forebrain; notably, its expression in the VP is greatly reduced after E14.5 [21]. Previous studies showed that neurons of the Dbx1-lineage contribute to PC [17,21,22]. Here, we first used a genetic model with an enlarged PC to demonstrate that the Dbx1 expression level is correlated with the size of PC. This suggests that neurons of the Dbx1 lineage are important contributors to the PC. Using $Dbx1^{Cre}$ to label neurons from the Dbx1 lineage, we confirmed that this population contributes significantly to the PC. We further characterized the distribution, morphology, and neurogenesis patterns of the PC neurons derived from the Dbx1 lineage and found these neurons show stereotypical distributions, timings of neurogenesis and output projection patterns. Our findings suggested that neuronal lineage might be a critical determinant of PC functional domains.

Results

The expression of *Dbx1* is correlated with the size of PC

A dramatic expansion of Dbx1 expression domain was previously reported in the dorsal telencephalon of *Lhx2* null mutant cortices [23]. As neurons derived from the *Dbx1* lineage contribute to the PC [17], and deletion of *Lhx2* in cortical progenitors by *Emx1*-Cre leads to the generation of ectopic piriform cortex [24], we further tested whether the expanded PC in *Lhx2* conditional knockout animals (*Lhx2* cKO;

Lhx2$^{f/f}$:*Emx1*^{Cre}) is correlated with an increase of *Dbx1* expression. We first confirmed that the expression of *Lhx2* is absent and the expression of *Pax6* is downregulated in the dorsal telencephalon of cKO cortices at E13.5, as shown previously [25]. We then compared the expression levels of *Dbx1* in control and *Lhx2* cKO cortices. By qPCR, we found that both *Dbx1* and *Reelin* (*Rln*), a marker for Cajal Retzius cells, which the *Dbx1* lineage contributes to [26], are significantly upregulated in the *Lhx2* cKO cortex (Figure 1a).

To confirm that the *Dbx1* expression pattern is expanded in *Lhx2* cKO mice, we crossed *Lhx2* cKO with the *Dbx1*^{LacZ} reporter line, which has a *LacZ* gene knocked-in to the *Dbx1* locus [18]. While LacZ-expressing cells are derived from the VP at pallial-subpallial boundary (PSB) in wild-type *Dbx1*^{LacZ} animals, we observed that the number of *Dbx1*-LacZ-expressing cells is dramatically increased in the *Lhx2* cKO at E13.5 (Figure 1b). Further, we found many LacZ+ cells were distributed throughout the cKO dorsal telencephalon (Figure 1b), in concordance with the dorsal expansion of the PC in *Lhx2* cKO mice. This correlation of increased production of *Dbx1*-lineage neurons and increased PC size in the *Lhx2* cKO suggests that the *Dbx1* lineage could contribute significantly to the PC.

***Dbx1*-lineage neurons in the piriform cortex are mostly excitatory neurons**

Next, we performed a basic characterization of the Dbx1-lineage neurons in the PC. First, we studied the distribution of Dbx1 neurons by dividing the PC into four sub-regions, including the dorsal and ventral portions of APC and PPC. As can be seen in Figure 2a, the APC appears as an elongated "S" shape in coronal sections of *Dbx1*^{Cre}:Ai3 (allowing permanent tracing of Dbx1-derivatives) cortex at P7. The dorsal and ventral portions of the APC were identified by the presence of the lateral olfactory tract (LOT) above L1 specifically in the ventral APC (vAPC). In contrast with the APC, the PPC does not have a superficial LOT, and its structure is more linear (Figure 2b). We further denote the dorsal and ventral halves of the PPC as dPPC and vPPC, respectively. After crossing the *Dbx1*^{Cre} mice [21] with the Ai3 reporter line to label *Dbx1*-derived cells with YFP, we measured the *Dbx1*-derived cell density in dorsal and ventral APC and PPC at P7. Cells derived from the *Dbx1* lineage contributed to about 8% of all PC cells. Further, in both APC and PPC, a significantly higher density of *Dbx1*- lineage cells (*Dbx1*-lineage cells

(green)/total cells labeled by DAPI) was found in the ventral regions, when compared with the corresponding dorsal regions (dAPC, 5.94 ± 0.41%; vAPC, 9.36 ± 0.32%; n = 3; $P = 0.0027$. dPPC, 8.32 ± 0.23%; vPPC, 10.09 ± 0.13%; n = 3; $P = 0.0025$) (Figure 2c).

As Dbx1 is also expressed in the preoptic area and the *Dbx1* lineage contributes to both excitatory and inhibitory neurons in the amygdala [27], we next determined what portion of the *Dbx1*-derived cells in the PC are GABAergic interneurons. To identify inhibitory interneurons among the *Dbx1*-derived cells in the PC, we crossed $Dbx1^{Cre}$:Ai14 mice, in which *Dbx1*-lineage cells are labeled with tdTomato, with the $Gad67^{GFP}$ transgenic line, where all GABAergic inhibitory interneurons are labeled with GFP [28]. At P30, we quantified the *Dbx1*-derived cells ($tdTomato^+$) and *Dbx1*-derived interneurons ($tdTomato^+GFP^+$) and calculated the percentage of *Dbx1*-lineage neurons that are interneurons (Figure 2d). We found a relatively low percentage (~4%) of *Dbx1*-derived cells to be GFP^+ across the PC (Figure 2e), suggesting that very few *Dbx1*-derived cells in the PC are GABAergic inhibitory neurons.

To complement this finding, we also examined the proportion of *Dbx1*-derived cells of the *Emx1*-lineage. Emx1 is expressed in cortical progenitors located in the ventricular zone of the dorsal telencephalon, and most of the excitatory projection neurons in the cerebral cortex are derived from this *Emx1* lineage [29]. As we could not label distinct lineages with two Cre lines in one animal, we used the $Dbx1^{LacZ}$ reporter line to trace cells of *Dbx1* lineage in $Emx1^{Cre}$: Ai14 cortices, where cells of *Emx1* lineage express tdTomato. At E12.5, we found that along the anterior/posterior axis, the majority of the *Dbx1*-$LacZ^+$ cells around the PSB (~80%) also express tdTomato (Figure S1). This high degree of colocalization suggests that most cells derived from *Dbx1* progenitors are excitatory neurons of the *Emx1* lineage.

Dbx1-lineage neurons show diverse neuronal morphology

We then defined cell type of the *Dbx1*-derived cells by their morphology. In the PC, several neuronal subtypes have been described based on their morphology, including horizontal cells in L1, semilunar cells and superficial pyramidal cells in

L2, and deep pyramidal cells and multipolar cells in L3 [30]. To examine the morphologies of *Dbx1*-lineage cells in the PC, we crossed *Dbx1*^{Cre} with Ai14 and utilized the strong tdTomato expression to characterize the morphology of *Dbx1*-derived cells at P30. Based on cellular morphology, we found at the stages we analyzed, very few *Dbx1*-derived cells are glia and the majority of them are neurons. As shown in Figure 3, the *Dbx1* lineage exhibits a variety of neuronal morphologies throughout the PC. Similar to the cell types reported in previous studies, we observed *Dbx1* cells with morphology of horizontal cells (H) and neuroglia (NG) in L1 (Figure 3a), semilunar cells (S) and superficial pyramidal cells (SPy) in L2 (Figure 3a, b), and deep pyramidal cells (DPy) and multipolar cells (M) in L3 (Figure 3a, b).

We then quantified the number of each neuronal type among the *Dbx1*-derived neurons. Although the *Dbx1*-derived cell density differed among different PC subregions, the composition of different cell types was consistent throughout the PC: In L1, the *Dbx1* cells were mostly neuroglia form and horizontal cells. In L2, about half the *Dbx1* cells were semilunar cells and the other half were superficial pyramidal cells. In L3, the *Dbx1* neurons were predominantly deep pyramidal cells and multipolar cells (Figure 3c).

Ventral distribution of *Dbx1*-derived neurons in the PC

We next wanted to determine how cells of the *Dbx1* lineage are distributed across the PC, so we collected serial coronal sections of P7 *Dbx1*^{Cre}:Ai3 cortices and quantified the number of YFP-expressing cells in the PC at eight evenly distributed planes along the anterior-posterior axis (as shown in Figure 4a, b). By comparing the total number of *Dbx1*-derived neurons in each section, we found most *Dbx1*-derived cells are located in the middle of the PC, including the caudal APC and rostral PPC (such as the sections 4 and 5 in Figure 4b). Additionally, more *Dbx1*-derived cells were found in the ventral PC compared to the dorsal regions (Figure 4b, c). Within a 300-μm-wide column, the number of *Dbx1* derived cells was roughly twice as high in the ventral PC than in the dorsal PC at many levels across the PC (Figure 4c). Thus, we found neurons of the *Dbx1* lineage show a preferential distribution toward the ventral PC.

We further analyzed the laminar distribution of *Dbx1*-derived cells in the PC by quantifying the percentage of *Dbx1*-derived cells in each layer of the PC. Although *Dbx1*-derived cells were found in all layers, most of them were found in L2 and L3 and more than 50% of the *Dbx1*-derived neurons were located in L2 at most levels (Figure 4d, e). In the dorsal APC, PPC and posterior ventral PPC, similar distribution of *Dbx1*-derived neurons in L2 and L3 was observed (Figure 4d, e). However, in the ventral APC, the *Dbx1*-derived neurons were highly enriched in the L2 (Figure 4e). .

Early generation of *Dbx1*-lineage cells

We further sought to delineate the developmental stages at which the *Dbx1* cells are generated. We injected EdU into pregnant mice at specific developmental time-points from E11.5 to E14.5 to label neurons generated at each stage. We first investigated the neurogenesis pattern of the general population of PC neurons, and we then compared it to the neurogenesis pattern of *Dbx1* derived PC neurons.

We analyzed the number and distribution of EdU^+ cells in the dorsal and ventral APC and PPC at P7. In agreement with previous studies [31], we found that neurogenesis is initiated by E11.5 in the PC (Figure 5a, b). Comparing the samples from different time-points, we found the number of cells produced decreases over time in all compartments of the PC. For example, significantly more cells were generated at E11.5, when compared to E12.5-E14.5 (Figure 5b) and much fewer cells were produced after E14.5. We also compared the laminar distribution of cells generated at each developmental stage. While the inside-out neurogenesis pattern was observed in the neocortex [32] (Figure S2), such pattern was not found in PC. Cells produced at E11.5 were distributed throughout L2 and L3 in PC, and most of the cells generated from E12.5 to E14.5 contributed to L2 (Figure 5a, c). More specifically, within L2, the earlier born cells were located more superficially than later born cells (Figure 5c) [31]. Further, we found the laminar distribution patterns of cells generated between E11.5 and E14.5 were similar among different domains in the PC (Figure 5c).

To analyze neurogenesis patterns, we labeled cells derived from the *Dbx1* lineage with YFP in *Dbx1*^{Cre}:Ai3 and injected EdU to label *Dbx1*-lineage cells generated between E11.5 and E14.5. We then analyzed the number and distribution of EdU-labeled YFP^{+} cells at P7. Compared to the general cell population in PC , most *Dbx1*-derived cells were generated at earlier time-points. The number of *Dbx1* cells produced also decreased over time in all compartments of the PC. When we compared the neurogenesis patterns of *Dbx1*-derived cells and the entire population of cells in PC, we found a significantly higher percentage of *Dbx1* cells generated at E11.5 in the APC (Figure 5d,e). For example, in the dorsal APC, about 20% of all cells are generated at E11.5, but a significantly higher percentage of *Dbx1* cells (about 35%) are generated at E11.5 (P = 0.000261, n = 3). Similarly, 27% of cells in the ventral APC are generated at E11.5, while a significantly higher percentage of Dbx1 cells (about 60%) in this region are generated at E11.5 (P = 0.000115, n = 3) (Figure 5d). Additionally, a much lower percentage of *Dbx1* cells across the PC are generated after E14.5, when compared with PC cells in general (Figure 5d, e). We found the distributions of *Dbx1* cells generated at specific stages were similar to PC cells in general; cells generated at E11.5 were distributed in both L2 and L3, while cells generated at and after E12.5 were more focused in L2 (Figure 5a, e).

Overall, the neuronal birthdating analyses demonstrated that cells of the *Dbx1* lineage generated between E11.5 and E14.5 show a similar distribution pattern as the general PC neuronal population. However, the *Dbx1* derived PC cells contribute mainly to the early-born population of PC cells; most of them were generated by E11.5 or E12.5, and almost no *Dbx1* derived cells were generated after E14.5.

Many Dbx1-derived neurons in the vAPC project to the orbitofrontal cortex

Next, we examined the efferent property of the *Dbx1*-lineage neurons.
Since neurons of the *Dbx1* lineage were preferentially distributed in the ventral PC (Figure 4) and orbitofrontal cortex-projecting neurons are also preferentially located in the ventral PC [13], we investigated whether *Dbx1* neurons preferentially project to the orbitofrontal cortex. A retrograde neural tracer, cholera toxin B subunit (CTB) coupled to green fluorescent dye, was injected into the lateral

orbitofrontal cortex (LO) of *Dbx1*^{Cre}:Ai14 mice (Figure 6a). In agreement with previous findings [13], we found many LO-projecting neurons (CTB$^+$) in the APC, with a majority located in the vAPC (Figure 6b, c). Interestingly, the majority of LO-projecting neurons in the vAPC were derived from the *Dbx1* lineage (CTB$^+$tdTomato$^+$) (Figure 6d). We quantified the number of CTB positive and CTB and tdTomato double positive neurons in the section containing the most CTB$^+$ neurons in the ventral APC. Among the general population of neurons in the vAPC, only about 4% were CTB$^+$ (number of CTB$^+$ cells/number of total cells, labeled by DAPI: 3.91 ± 0.20%) (Figure 6e). However, a significant higher proportion of neurons of the *Dbx1* neuronal lineage (tdTomato+) were CTB+ (number of CTB$^+$tdTomato$^+$/number of tdTomato$^+$ cells: 58.13 ± 2.29%; $P <$ 0.001, n = 3, when compared to the general population of neurons in the vAPC) (Figure 6e). This finding suggested that neurons of *Dbx1* lineage in the vAPC preferentially project to the orbitofrontal cortex.

Discussion

PC has long been considered synonymous with the primary olfactory cortex [33] as it is a critical brain region for processing external chemical signals and influencing perception, emotion, learning and memory, and it delivers odor information to higher centers, such as the prefrontal cortex, hippocampus and amygdaloid areas [34]. In this study, we analyzed the contribution of *Dbx1*-lineage neurons to the PC. In the spinal cord, differential regional expression of *Dbx1* along the ventral-dorsal axis is known to be critical for the differentiation of V0 and V1 neuronal fate [18]. *Dbx1* is also expressed in a specific progenitor population in the VP at the PSB [21]. We showed that very few *Dbx1*-lineage cells in the PC are interneurons or glia. Although *Dbx1*-derived cells are found in all layers of the PC across the anterior-posterior axis, and the neurons exhibit layer-specific idiosyncratic neuronal morphologies, we identified a distinct generation time-point for *Dbx1*-lineage cells, which corresponds to their most frequent laminar fate in the PC. We found *Dbx1*-lineage cells were born earlier among the PC neuronal population. As neuronal birthdates were shown to determine neuronal physiology and connectivity in the dentate gyrus [35], the neuronal birthdating results for *Dbx1*-derived neurons suggested that these cells might have specialized roles in the PC. A specific function for *Dbx1*-lineage neurons was further suggested by their distribution

preferences, i.e., we found the *Dbx1*-cell number peaks at the middle of PC and they were enriched in L2 and the ventral PC. Further, the *Dbx1*-lineage neurons in the ventral APC show a significant preference projecting to the lateral orbitofrontal cortex. Thus, our findings that neurons derived from the *Dbx1* lineage show a preferred distribution, timing of neurogenesis and output projection pattern, suggest that these cells might contribute to a specific PC neuronal population or specific function of the PC.

The differential distribution of *Dbx1*-lineage neurons in different PC subregions could partially contribute to the different functions in these PC subregions. The demarcation of the PC into subregions with functional differences was hypothesized decades ago [36,37]. However, this topic has been minimally explored. The APC was initially divided into dorsal and ventral regions based on structural differences, such as the presence of the LOT in the vAPC. Additionally, specific stimulation of these two regions elicited different physiological outcomes [9,36,37]. In particular, a deep region in the ventral APC was found to be a sensitive area for stimulation-evoked seizures [38]. Our findings that in general, neurons in vAPC are generated earlier than that in dAPC and that the cells of the *Dbx1* lineage in vAPC are generated early among the overall vAPC cell population suggest that the timing of neurogenesis might also contribute to the functional demarcation between PC subregions.

A related open question is how the PC processes olfaction. In the olfactory bulb, each mitral and tufted cell sends a single dendrite to its respective glomerulus, and sends axon collaterals to multiple higher brain areas, including the PC [4,39]. Individual PC neurons receive projection from mitral and tufted cells all over the OB, making odor representations in the PC not only spatially distributed but also spatially mingled with one another [5,40]. With afferent circuit highly distributed, a recent study revealed that efferent circuit of the PC appears to be topographically organized [13]. Chen and colleagues show that PC neurons with different orbitofrontal targets have distinct and stereotypic distribution patterns across the PC and these two neuronal populations overlap minimally. This finding suggested that neurons with the same output targets might serve as a functional unit of the PC. However, what mechanisms determine these output projection patterns of PC

neurons were previously unknown. Our findings suggest that neuronal lineage/origin might be an important determinant of efferent projection patterns for PC neurons. This idea is consistent with a previous hypothesis that the connectivity of PC neurons is specified by neuronal molecular identity [41].

Taken together, the preference of Dbx1-lineage neurons for ventral distribution, early neurogenesis and typical projection output to the lateral orbitofrontal cortex suggests that functional properties of PC neurons might be determined partly by lineage. Similar to the findings for PC afferent neurons that similar cell types target similar areas in the PC [42], we showed that neurons of the same lineage are likely to project to the same region. Our study here provides a better understanding of PC organization, and it could ultimately contribute to the understanding the neural mechanisms underlying odor percept formation.

Methods

Mouse lines

Dbx1^{LacZ} [18] and *Dbx1*^{Cre} [21] mouse lines were kindly provided by Dr. Alessandra Pierani. Lhx2 floxed, *Emx1*^{Cre} and Gad67-GFP mice were kindly provided by Drs. Dennis O'Leary [24], Kevin Jones [29], and Yuchio Yanagawa [28]. Additional reporter lines, such as Ai3 [Gt(ROSA)26Sor$^{tm3(CAG-EYFP)Hze}$] and Ai14 [Gt(ROSA)26Sor$^{tm14(CAG-tdTomato)Hze}$] [43], were used. Animal care and experimental procedures were approved by and performed in accordance with guidelines provided by the Academia Sinica Institutional Animal Care and Use Committee. The day of identifying a vaginal plug and the day of birth were respectively designated as embryonic day 0.5 (E0.5), and postnatal day 0 (P0).

Quantitative RT-PCR

RNA samples were isolated from E13.5 dorsal telencephalon using TriPure Isolation Reagent (Roche) and treated with DNaseI (Promega) to eliminate genomic DNA. First-strand cDNA was synthesized from 1 μg total RNA using Transcriptor First Strand cDNA Synthesis Kit (Roche), and 0.2 μl cDNA was used for each quantitative PCR reaction. Real-time RT-PCR was performed using LightCycler® 480 SYBR Green I Master mix (Roche). Gene expression was

normalized to GAPDH and data were analyzed by two-tailed, unpaired *t*-test with Welch's correction.

Primers used for qPCR:
GAPDH, F: GGCAAATTCAACGGCACAG, R:
CGGAGATGATGACCCTTTGG;
Lhx2, F: GCATCTACTGCAAAGAAGACTACTACA, R:
CGCATCACCATCTCT GAGG; Pax6, F:
GCCCTTCCATCTTTGCTTGGGAAA, R: TAGCCAGGTTGGGA
AGAACTCTG; Reelin, F: AACCACGGCCTTACATGG, R:
GTAAATTCCTGGCA GCTTGG; Dbx1, F: CAACAGACCCACCACCTTCT, R:
AGGAGCTGGCACTCTG AAA.

Immunohistochemistry and EdU labeling

Timed-pregnant mice were dissected, and embryonic cortices were fixed in 4% phosphate-buffered paraformaldehyde (PFA); postnatal brains were perfused with and postfixed in 4% PFA. For histological analyses, brains were cryoprotected with 30% sucrose in PBS, embedded in Tissue-Tek OCT compound (Sakura Finetek) and cut in 20-25 μm sections on a cryostat (Leica). Immunohistochemistry was performed as described [24]. In short, primary antibodies, including chick anti-mCherry (Abcam, ab205402, 1:500) and anti-GFP (Torey Pines Biolabs, TP-401, 1:500) were incubated overnight at 4°C in blocking solution containing 3% BSA (Sigma-Aldrich) and 0.3% Triton X-100 in phosphate buffer, followed by incubation with Alexa-conjugated secondary antibodies (Jackson ImmunoResearch) for 2 h at room temperature. Cell nuclei were counterstained with DAPI (Vector). Neuronal birthdating analyses were performed as described [44]. Briefly, EdU (500 ng) was injected into timed-pregnant mice, and the EdU-positive cells were detected with a Click-iT EdU imaging kit (Life Technologies).

CTB tracing

Animals (young male *Dbx1*^{Cre}:Ai14 mice on a C57BL/6J background; ~30 g, 4-5 weeks old) were anesthetized by injecting ketamine/xylazine (initial dose, 90

mg/10 mg/kg) intraperitoneally. A deeply anesthetized animal was placed into a stereotaxic device with a heating unit. One burr hole (~3 mm × 2 mm) was drilled on the dorsal surface of the skull. Dura mater was carefully removed using a new 19 G needle. The injection micropipette was pulled from glasses capillaries (OD, 1.14 mm; ID, 0.53 mm, Drummond Scientific Company) with an opening of ~20 μm in diameter. The micropipette installed onto a pressure injector (Nanoject III, Drummond Scientific Company) was loaded with 0.5% CTB, Alexa Fluor 488 conjugate (ThermoFisher Scientific) in phosphate buffer saline (pH 7.4). The micropipette tip was then positioned into the LO (2.46 mm anterior and 1.25 mm lateral to bregma and 1.50 mm from the surface) to deliver 50 nl of CTB solution at the speed of 1 nl /second.

Quantification and statistical analyses

In general, 300-μm-wide cortical columns were cropped for quantification of cell numbers and marker intensity. The numbers of YFP^+, $tdTomato^+$, and EdU^+ cells were manually counted using ImageJ FIJI. All analyses were performed with three or more biological replicates. The number of individual animals of the same genotype used is indicated as "n" in the text and figures. Statistical analyses were performed using GraphPad Prism 5 software. All quantitative data are presented as the mean ± SEM. Minimal statistical significance was fixed at $P < 0.05$ for comparisons made by unpaired t-test with Welch's correction. Significance is represented in figures as: *, $P < 0.05$; **, $P < 0.01$; ***, $P < 0.001$.

Acknowledgements We thank members of the Chou laboratory for their help. This work was supported by Ministry of Science and Technology of Taiwan (MOST 104-2311-B-001-031-MY3, SJC; MOST 105-3111-Y-016-003, CFC), Academia Sinica (AS-CDA-107-L09, SJC), the Institute of Cellular and Organismic Biology of Academia Sinica (SJC).

Conflict of Interest None of the authors has any financial or non-financial conflicts related to this work.

Author contributions: S-J.C. designed the research; T.S., H-L.C. and Z-h.Z. performed the research and analyzed data; A.P. provided critical materials; C-F.C. and S-J.C. wrote the paper.

References

1 Doty, R. L. Odor-guided behavior in mammals. *Experientia* **42**, 257-271 (1986).

2 Mombaerts, P. *et al.* Visualizing an olfactory sensory map. *Cell* **87**, 675-686 (1996).

3 Miyamichi, K. *et al.* Cortical representations of olfactory input by trans-synaptic tracing. *Nature* **472**, 191-196, doi:10.1038/nature09714 (2011).

4 Sosulski, D. L., Bloom, M. L., Cutforth, T., Axel, R. & Datta, S. R. Distinct representations of olfactory information in different cortical centres. *Nature* **472**, 213-216, doi:10.1038/nature09868 (2011).

5 Rennaker, R. L., Chen, C. F., Ruyle, A. M., Sloan, A. M. & Wilson, D. A. Spatial and temporal distribution of odorant-evoked activity in the piriform cortex. *J Neurosci* **27**, 1534-1542, doi:10.1523/JNEUROSCI.4072-06.2007 (2007).

6 Kay, R. B., Meyer, E. A., Illig, K. R. & Brunjes, P. C. Spatial distribution of neural activity in the anterior olfactory nucleus evoked by odor and electrical stimulation. *J Comp Neurol* **519**, 277-289, doi:10.1002/cne.22519 (2011).

7 Xu, W. & Wilson, D. A. Odor-evoked activity in the mouse lateral entorhinal cortex. *Neuroscience* **223**, 12-20, doi:10.1016/j.neuroscience.2012.07.067 (2012).

8 Root, C. M., Denny, C. A., Hen, R. & Axel, R. The participation of cortical amygdala in innate, odour-driven behaviour. *Nature* **515**, 269-273, doi:10.1038/nature13897 (2014).

9 Ekstrand, J. J. *et al.* A new subdivision of anterior piriform cortex and associated deep nucleus with novel features of interest for olfaction and epilepsy. *J Comp Neurol* **434**, 289-307, doi:DOI 10.1002/cne.1178 (2001).

10 Illig, K. R. Projections from orbitofrontal cortex to anterior piriform cortex in the rat suggest a role in olfactory information processing. *J Comp Neurol* **488**, 224-231, doi:10.1002/cne.20595 (2005).

11 Nagayama, S. *et al.* Differential axonal projection of mitral and tufted cells in the mouse main olfactory system. *Front Neural Circuit* **4**, doi:ARTN 120 10.3389/fncir.2010.00120 (2010).

12 Luskin, M. B. & Price, J. L. The topographic organization of associational fibers of the olfactory system in the rat, including centrifugal fibers to the olfactory bulb. *J Comp Neurol* **216**, 264-291, doi:10.1002/cne.902160305 (1983).

13 Chen, C. F. F. *et al.* Nonsensory target-dependent organization of piriform cortex. *Proceedings of the National Academy of Sciences of the*

United States of America **111**, 16931-16936, doi:10.1073/pnas.1411266111 (2014).
14 Valverde, F. Posterior Column Nuclei and Adjacent Structures in Rodents - a Correlated Study by Golgi Method and Electron Microscopy. *Anat Rec* **151**, 496-& (1965).
15 Carney, R. S. *et al.* Cell migration along the lateral cortical stream to the developing basal telencephalic limbic system. *J Neurosci* **26**, 11562-11574, doi:10.1523/JNEUROSCI.3092-06.2006 (2006).
16 Garcia-Moreno, F., Lopez-Mascaraque, L. & de Carlos, J. A. Early telencephalic migration topographically converging in the olfactory cortex. *Cereb Cortex* **18**, 1239-1252, doi:10.1093/cercor/bhm154 (2008).
17 Puelles, L. *et al.* Radial derivatives of the mouse ventral pallium traced with Dbx1-LacZ reporters. *J Chem Neuroanat* **75**, 2-19, doi:10.1016/j.jchemneu.2015.10.011 (2016).
18 Pierani, A. *et al.* Control of interneuron fate in the developing spinal cord by the progenitor homeodomain protein Dbx1. *Neuron* **29**, 367-384, doi:10.1016/s0896-6273(01)00212-4 (2001).
19 Bouvier, J. *et al.* Hindbrain interneurons and axon guidance signaling critical for breathing. *Nat Neurosci* **13**, 1066-1074, doi:10.1038/nn.2622 (2010).
20 Sokolowski, K. *et al.* Specification of select hypothalamic circuits and innate behaviors by the embryonic patterning gene dbx1. *Neuron* **86**, 403-416, doi:10.1016/j.neuron.2015.03.022 (2015).
21 Bielle, F. *et al.* Multiple origins of Cajal-Retzius cells at the borders of the developing pallium. *Nat Neurosci* **8**, 1002-1012, doi:10.1038/nn1511 (2005).
22 Teissier, A. *et al.* A Novel Transient Glutamatergic Population Migrating from the Pallial-Subpallial Boundary Contributes to Neocortical Development. *J Neurosci* **30**, 10563-10574, doi:10.1523/Jneurosci.0776-10.2010 (2010).
23 Mangale, V. S. *et al.* Lhx2 selector activity specifies cortical identity and suppresses hippocampal organizer fate. *Science* **319**, 304-309, doi:10.1126/science.1151695 (2008).
24 Chou, S. J., Perez-Garcia, C. G., Kroll, T. T. & O'Leary, D. D. Lhx2 specifies regional fate in Emx1 lineage of telencephalic progenitors generating cerebral cortex. *Nat Neurosci* **12**, 1381-1389, doi:10.1038/nn.2427 (2009).
25 Hsu, L. C. *et al.* Lhx2 regulates the timing of beta-catenin-dependent cortical neurogenesis. *Proc Natl Acad Sci U S A* **112**, 12199-12204, doi:10.1073/pnas.1507145112 (2015).
26 Griveau, A. *et al.* A novel role for Dbx1-derived Cajal-Retzius cells in early regionalization of the cerebral cortical neuroepithelium. *PLoS Biol* **8**, e1000440, doi:10.1371/journal.pbio.1000440 (2010).
27 Hirata, T. *et al.* Identification of distinct telencephalic progenitor pools for neuronal diversity in the amygdala. *Nat Neurosci* **12**, 141-149, doi:10.1038/nn.2241 (2009).
28 Tamamaki, N. *et al.* Green fluorescent protein expression and colocalization with calretinin, parvalbumin, and somatostatin in the

GAD67-GFP knock-in mouse. *J Comp Neurol* **467**, 60-79, doi:10.1002/cne.10905 (2003).
29 Gorski, J. A. *et al.* Cortical excitatory neurons and glia, but not GABAergic neurons, are produced in the Emx1-expressing lineage. *J Neurosci* **22**, 6309-6314, doi:20026564 (2002).
30 Neville KR, H. L. *Olfactory cortex. The synaptic organization of the brain.* . 5th edn, (Oxford University Press, 2004).
31 Martin-Lopez, E., Ishiguro, K. & Greer, C. A. The Laminar Organization of Piriform Cortex Follows a Selective Developmental and Migratory Program Established by Cell Lineage. *Cereb Cortex*, 1-16, doi:10.1093/cercor/bhx291 (2017).
32 Dwyer, N. D. *et al.* Neural Stem Cells to Cerebral Cortex: Emerging Mechanisms Regulating Progenitor Behavior and Productivity. *J Neurosci* **36**, 11394-11401, doi:10.1523/JNEUROSCI.2359-16.2016 (2016).
33 Yeshurun, Y. & Sobel, N. An odor is not worth a thousand words: from multidimensional odors to unidimensional odor objects. *Annu Rev Psychol* **61**, 219-241, C211-215, doi:10.1146/annurev.psych.60.110707.163639 (2010).
34 Johnson, D. M., Illig, K. R., Behan, M. & Haberly, L. B. New features of connectivity in piriform cortex visualized by intracellular injection of pyramidal cells suggest that "primary" olfactory cortex functions like "association" cortex in other sensory systems. *J Neurosci* **20**, 6974-6982 (2000).
35 Save, L., Baude, A. & Cossart, R. Temporal Embryonic Origin Critically Determines Cellular Physiology in the Dentate Gyrus. *Cereb Cortex* **29**, 2639-2652, doi:10.1093/cercor/bhy132 (2019).
36 Kawaguchi, K. & Simon, R. P. Deep prepiriform cortex modulates neuronal cell death in global ischemia. *J Cereb Blood Flow Metab* **17**, 356-360, doi:10.1097/00004647-199703000-00012 (1997).
37 Shimosaka, S., So, Y. T. & Simon, R. P. Deep Prepiriform Cortex Modulates Kainate-Induced Hippocampal Injury. *Neuroscience* **61**, 817-822, doi:Doi 10.1016/0306-4522(94)90404-9 (1994).
38 Piredda, S. & Gale, K. A Crucial Epileptogenic Site in the Deep Prepiriform Cortex. *Nature* **317**, 623-625, doi:DOI 10.1038/317623a0 (1985).
39 Wilson, D. A. & Stevenson, R. J. *Learning to smell : olfactory perception from neurobiology to behavior*. (Johns Hopkins University Press, 2006).
40 Stettler, D. D. & Axel, R. Representations of odor in the piriform cortex. *Neuron* **63**, 854-864, doi:10.1016/j.neuron.2009.09.005 (2009).
41 Diodato, A. *et al.* Molecular signatures of neural connectivity in the olfactory cortex. *Nature Communications* **7**, doi:ARTN 1223810.1038/ncomms12238 (2016).
42 Wang, L. *et al.* Cell-Type-Specific Whole-Brain Direct Inputs to the Anterior and Posterior Piriform Cortex. *Front Neural Circuits* **14**, 4, doi:10.3389/fncir.2020.00004 (2020).

43 Madisen, L. *et al.* A robust and high-throughput Cre reporting and characterization system for the whole mouse brain. *Nat Neurosci* **13**, 133-140, doi:10.1038/nn.2467 (2010).
44 Hsing, H. W., Zhuang, Z. H., Niou, Z. X. & Chou, S. J. Temporal Differences in Interneuron Invasion of Neocortex and Piriform Cortex during Mouse Cortical Development. *Cereb Cortex*, doi:10.1093/cercor/bhz291 (2019).

Figure legends:

Figure 1. Dbx1 is upregulated in Lhx2 conditional knockout cortices. (a) Demonstrated by qPCR, the expression levels of *Lhx2* and *Pax6* are significantly downregulated in the cKO ($Lhx2^{f/f}$; $Emx1^{Cre}$) cortex when compared with WT ($Lhx2^{fl/+}$) at E13.5, while the levels of *Dbx1* and *Rln* are significantly upregulated in the cKO mice (n = 3-5; *Lhx2*, $P < 0.001$; *Pax6*, $P = 0.0054$; *Dbx1*, $P = 0.0085$; *Rln*, $P = 0.0412$). (b) LacZ staining on coronal sections of $Dbx1^{LacZ}$ cortices of WT (top) and cKO (bottom) embryos at E13.5. From anterior (A) to posterior (P), $LacZ^+$ cells (blue) are specifically located in the pallial-subpallial boundary (PSB, arrowheads) in WT. An increased number of $LacZ^+$ cells (indicated by unfilled arrowheads) was observed in the neocortex (NCx) of the cKO. Scale bar, 200 μm. GE, ganglionic eminence.

Figure 2. The contribution of cells of the *Dbx1* lineage in piriform cortex. (a, b) Coronal sections of $Dbx1^{Cre}$:Ai3 cortex at P7. Cells of the *Dbx1* lineage were labeled by YFP and are shown at the level of the anterior piriform cortex (APC) and posterior PC (PPC), as indicated on the left. The APC and PPC are further divided into dorsal and ventral subregions. (c) Density of cells of the *Dbx1* lineage (number of YFP+ cells/number of total cells) measured in a radial column in PC subregions. *Dbx1* cell denisty is significantly higher in ventral PC regions. (d) Coronal sections at the level of the APC from $Dbx1^{Cre}$:Ai14:$Gad67^{GFP}$ cortex at P30. Cells of *Dbx1* lineage were labeled by tdTomato and inhibitory interneurons were labeled by GFP. GFP- and tdTomato-positive cells are indicated by green and white arrowheads respectively, while double-labeled cells are indicated by yellow arrowheads. (e) Quantification of the percentage of interneurons in the Dbx1 lineage (number of $GFP^+tdTomato^+$ cells/number of $tdTomato^+$ cells). About 4% of the *Dbx1* lineage cells are inhibitory interneurons, across the PC. LOT, lateral olfactory tract; OB, olfactory bulb; NC, neocortex; Hp, hippocampus. Scale bars, 500μm (a) and 100μm (d).

Figure 3. Morphology of neurons of the *Dbx1* lineage. (a, b) Morphology of neurons of the *Dbx1* lineage was observed in coronal sections of $Dbx1^{Cre}$:Ai14 cortices at P30 at the levels of APC (a) and PPC (b) Images of insets are shown on

the right at higher magnification. Different cell types, as indicated, were identified based on their morphology. (c) Quantification of the percentage of each cell type observed in different sub-regions across PC. Scale bar, 100μm.

Figure 4. Neurons of the *Dbx1* lineage show preference to distribute in ventral PC and in layer 2. (a, b) Coronal sections of *Dbx1*^{Cre}:Ai3 cortex at P7 at eight levels from anterior (A) to posterior (P). (c) Quantification of the number of YFP-expressing cells in dorsal and ventral PC at each level. Higher numbers of YFP$^+$ cells were found in the ventral PC compared to dorsal PC. (d, e) Quantification of laminar distribution of YFP$^+$ cells. Most YFP$^+$ cells were detected in layer 2 (L2), across the PC. Scale bar, 100μm.

Figure 5. Neurons of the *Dbx1* lineage are early born neurons in PC. (a) YFP (cells of the *Dbx1* lineage, green) and EdU staining (red) in coronal sections from P7 *Dbx1*^{Cre}:Ai3 mice. EdU was injected into pregnant mothers at indicated stages. (b-e) Quantification of results from (a), indicating the numbers and distributions of EdU$^+$ cells (b, c) and EdU$^+$YFP$^+$ cells (d, e) at the indicated stages (n = 3). Scale bar, 100μm.

Figure 6. Neurons of the *Dbx1* lineage in the ventral APC preferentially project to orbitofrontal cortex. (a) Green fluorescence (Alexa Fluor 488)-conjugated CTB was injected into the lateral orbitofrontal cortex (LO) in *Dbx1*^{Cre}:Ai14 mice at P30. An injection site is shown in the coronal section (below). (b) CTB-labeled neurons (green) were detected throughout the APC (sections 1-4 from anterior to posterior). Neurons of the *Dbx1* lineage were labeled by tdTomato (Tom+, red). (c) Significantly more CTB-labeled neurons were detected in the ventral APC than in the dorsal APC. (d) LO-projecting neurons (green) were enriched in L2 of the ventral APC. Green-only neurons are indicated by hollow arrowheads and yellow neurons (positive for both green and red) are indicated by solid arrowheads. (e) Among the total population of neurons in vAPC L2 (labeled by DAPI), about 4% were LO projection neurons (labeled by CTB). Significantly higher percentage of LO-projecting neurons was found within the

neuronal population of the *Dbx1* lineage (more than 50%). Scale bar, 500μm (a), 100μm (b) and 50μm (d).

Figure 1

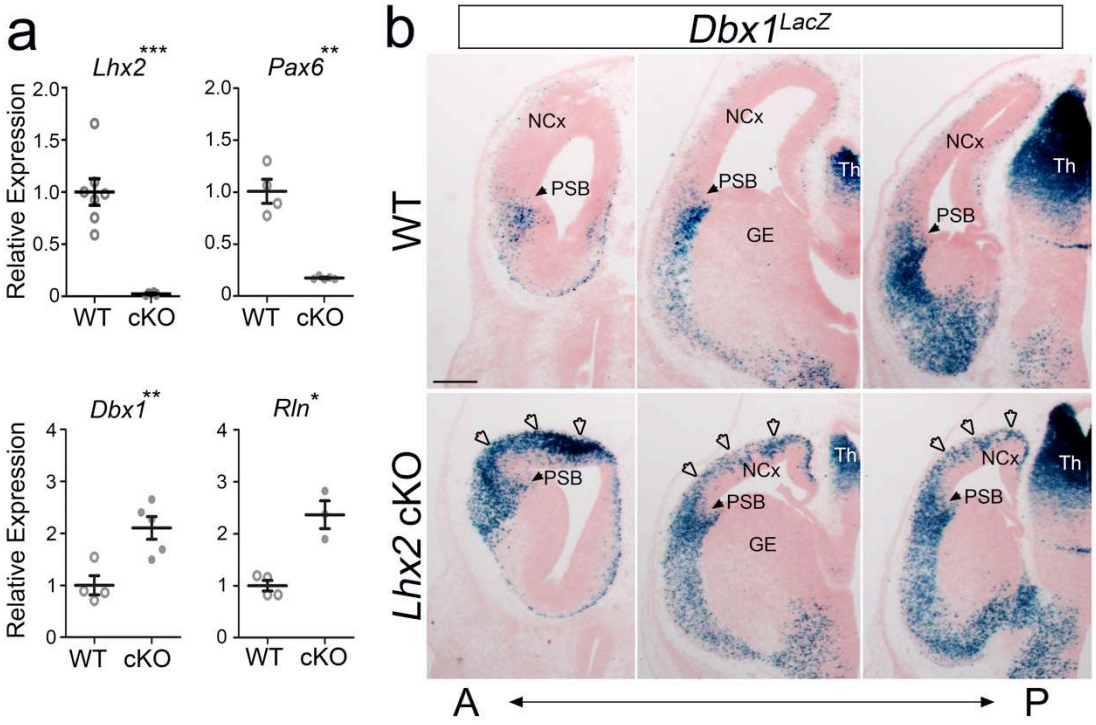
a
Lhx2***
Pax6**
Dbx1**
Rln*
Relative Expression
2.0
1.5
1.0
0.5
0
4
3
2
1
WT
cKO
b
Dbx1LacZ
WT
Lhx2 cKO
NCx
PSB
GE
Th
A
P

Figure 2

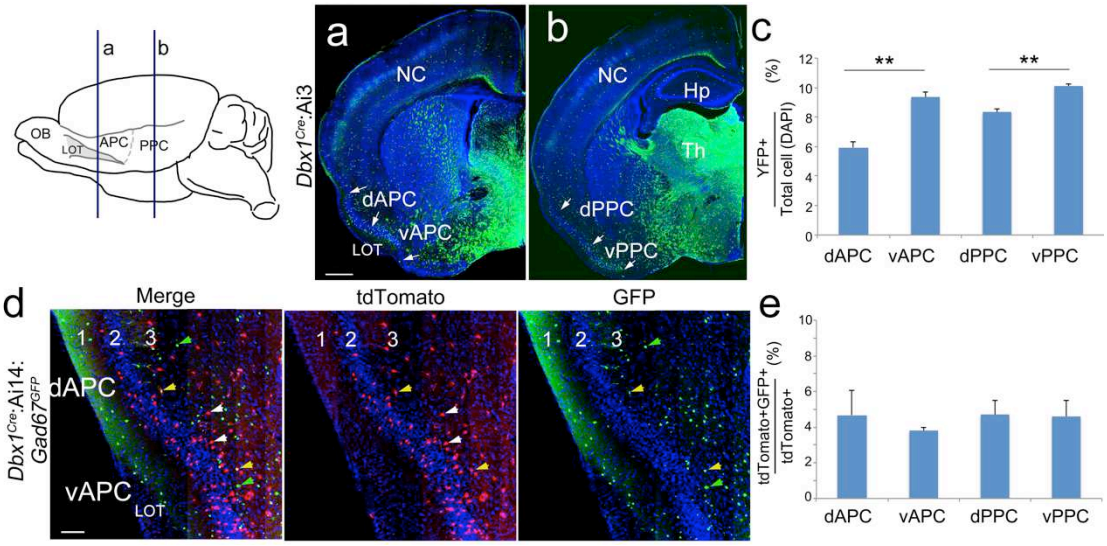
a
b
OB
LOT
APC
PPC
Dbx1Cre:Ai3
NC
dAPC
vAPC
LOT
Hp
Th
dPPC
vPPC
c
**
**
YFP+ / Total cell (DAPI) (%)
dAPC
vAPC
dPPC
vPPC
d
Merge
tdTomato
GFP
Dbx1Cre:Ai14:
Gad67GFP
1 2 3
dAPC
vAPC
LOT
e
tdTomato+GFP+ / tdTomato+ (%)
dAPC
vAPC
dPPC
vPPC

Figure 3

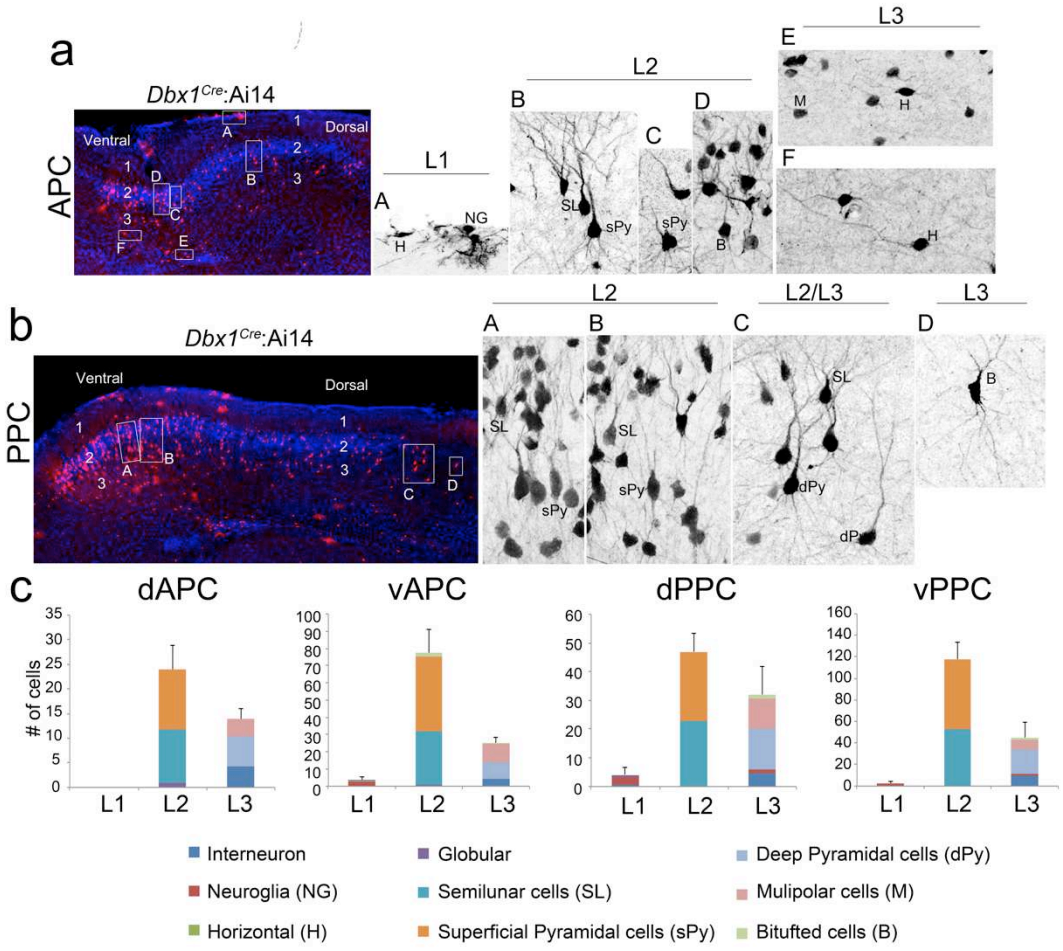
a
Dbx1Cre:Ai14
APC
Ventral
Dorsal
L1
L2
L3
b
Dbx1Cre:Ai14
PPC
L2/L3
c
dAPC
vAPC
dPPC
vPPC
# of cells
Interneuron
Globular
Deep Pyramidal cells (dPy)
Neuroglia (NG)
Semilunar cells (SL)
Mulipolar cells (M)
Horizontal (H)
Superficial Pyramidal cells (sPy)
Bitufted cells (B)

Figure 4

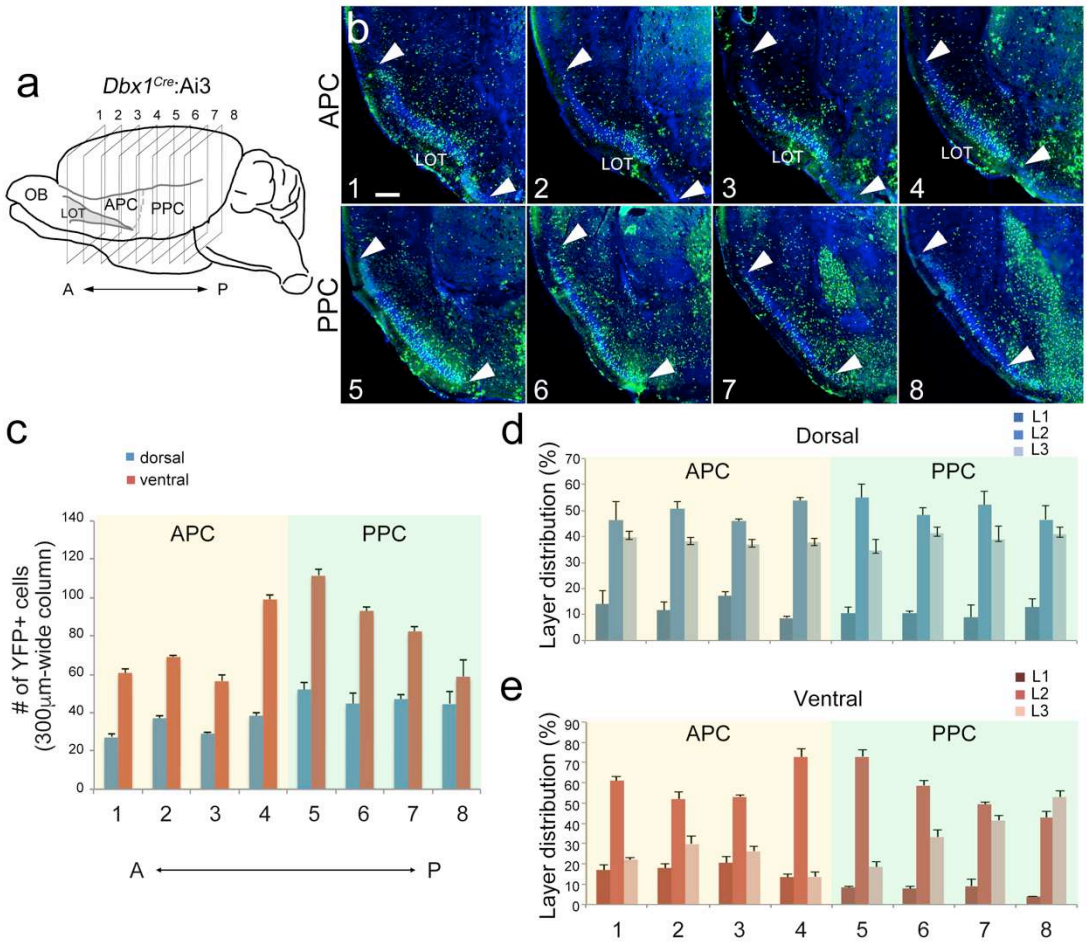
a
Dbx1Cre:Ai3
1 2 3 4 5 6 7 8
OB
LOT
APC
PPC
A
P
b
APC
PPC
LOT
1
2
3
4
5
6
7
8
c
dorsal
ventral
# of YFP+ cells (300μm-wide column)
APC
PPC
A
P
d
Dorsal
L1
L2
L3
Layer distribution (%)
e
Ventral

Figure 5

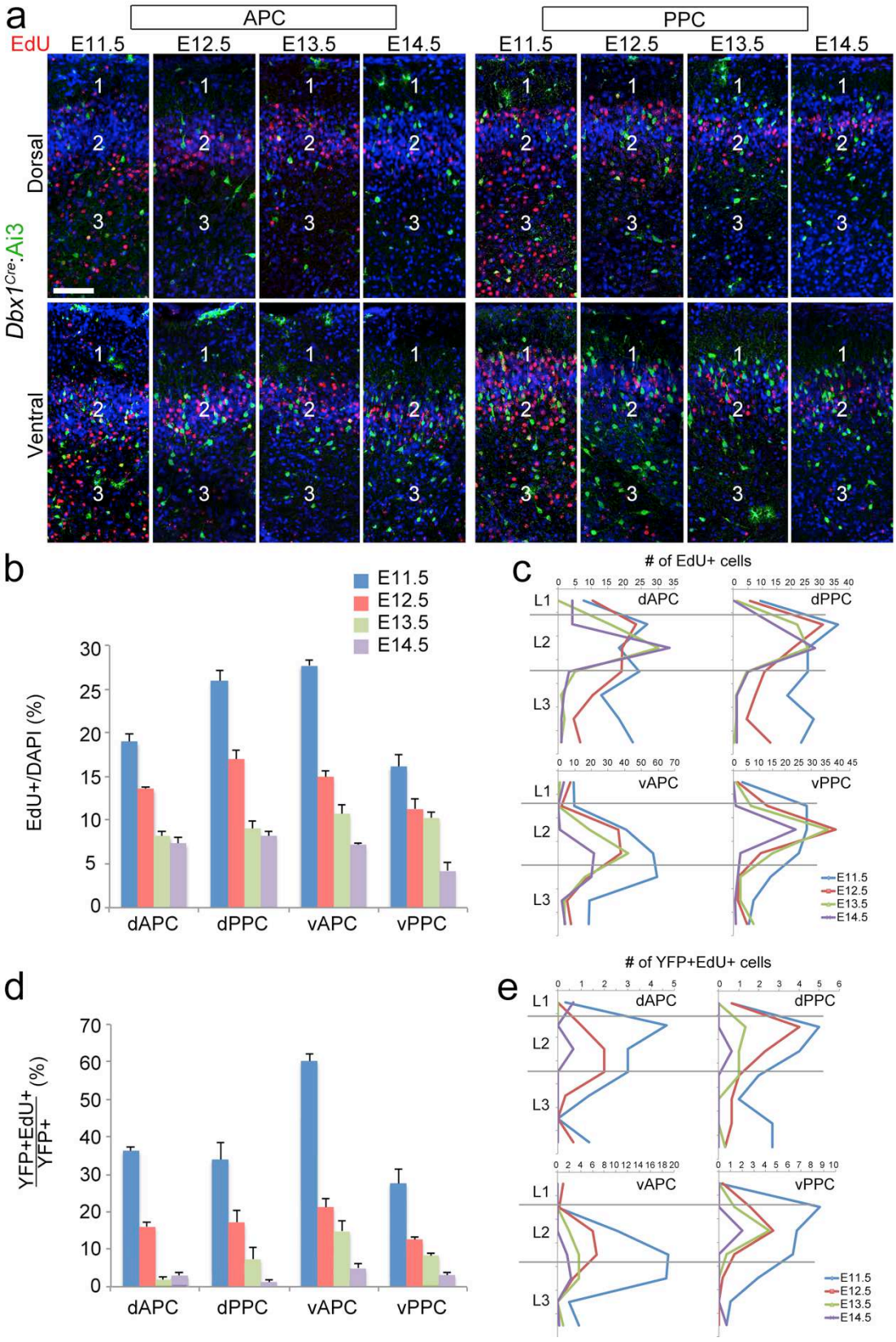
a
APC
PPC
EdU
E11.5
E12.5
E13.5
E14.5
Dorsal
Ventral
Dbx1Cre:Ai3
1
2
3
b
E11.5
E12.5
E13.5
E14.5
EdU+/DAPI (%)
dAPC
dPPC
vAPC
vPPC
c
# of EdU+ cells
L1
L2
L3
dAPC
dPPC
vAPC
vPPC
d
YFP+EdU+/YFP+ (%)
e
# of YFP+EdU+ cells

Figure 6

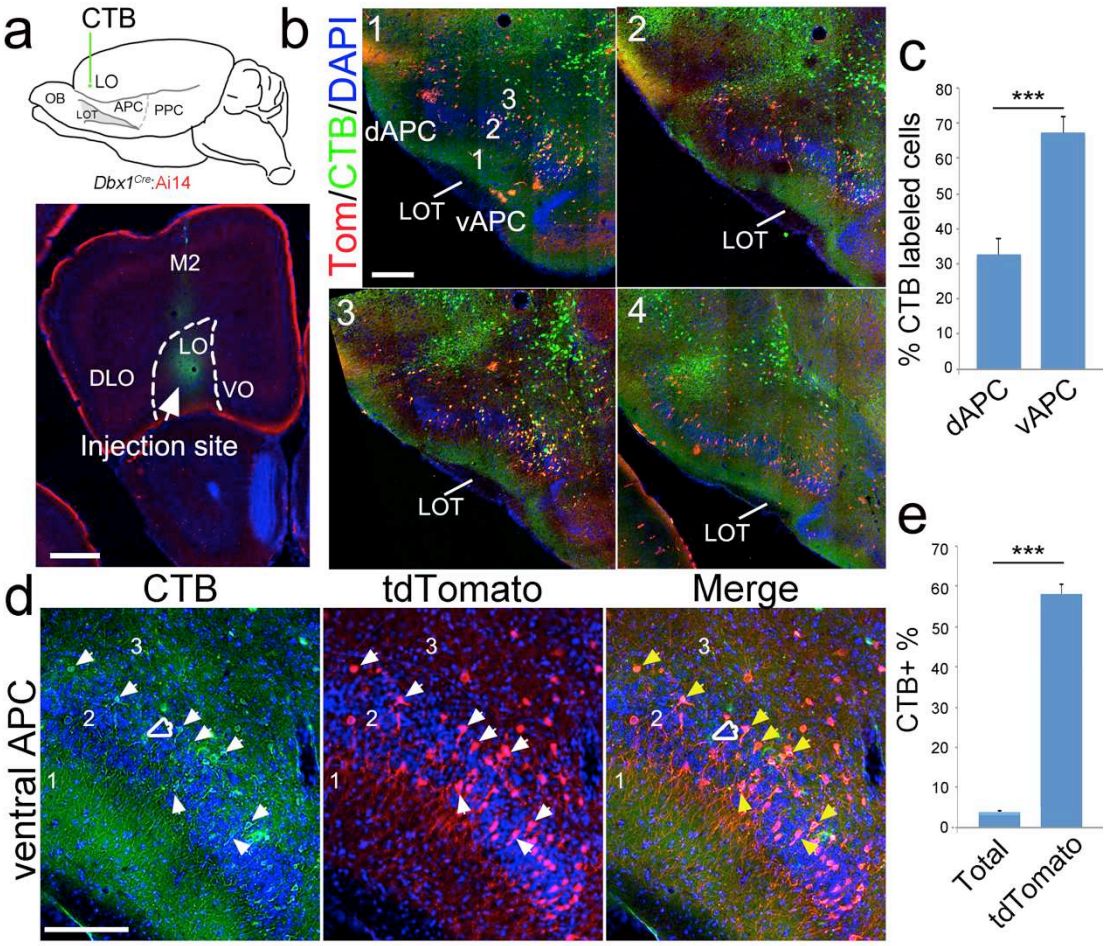
a
CTB
LO
OB
LOT
APC
PPC
Dbx1Cre:Ai14
M2
LO
DLO
VO
Injection site
b
Tom/CTB/DAPI
1
2
3
dAPC
LOT
vAPC
4
c
% CTB labeled cells
***
dAPC
vAPC
d
CTB
tdTomato
Merge
ventral APC
e
CTB+ %
***
Total
tdTomato

Figures

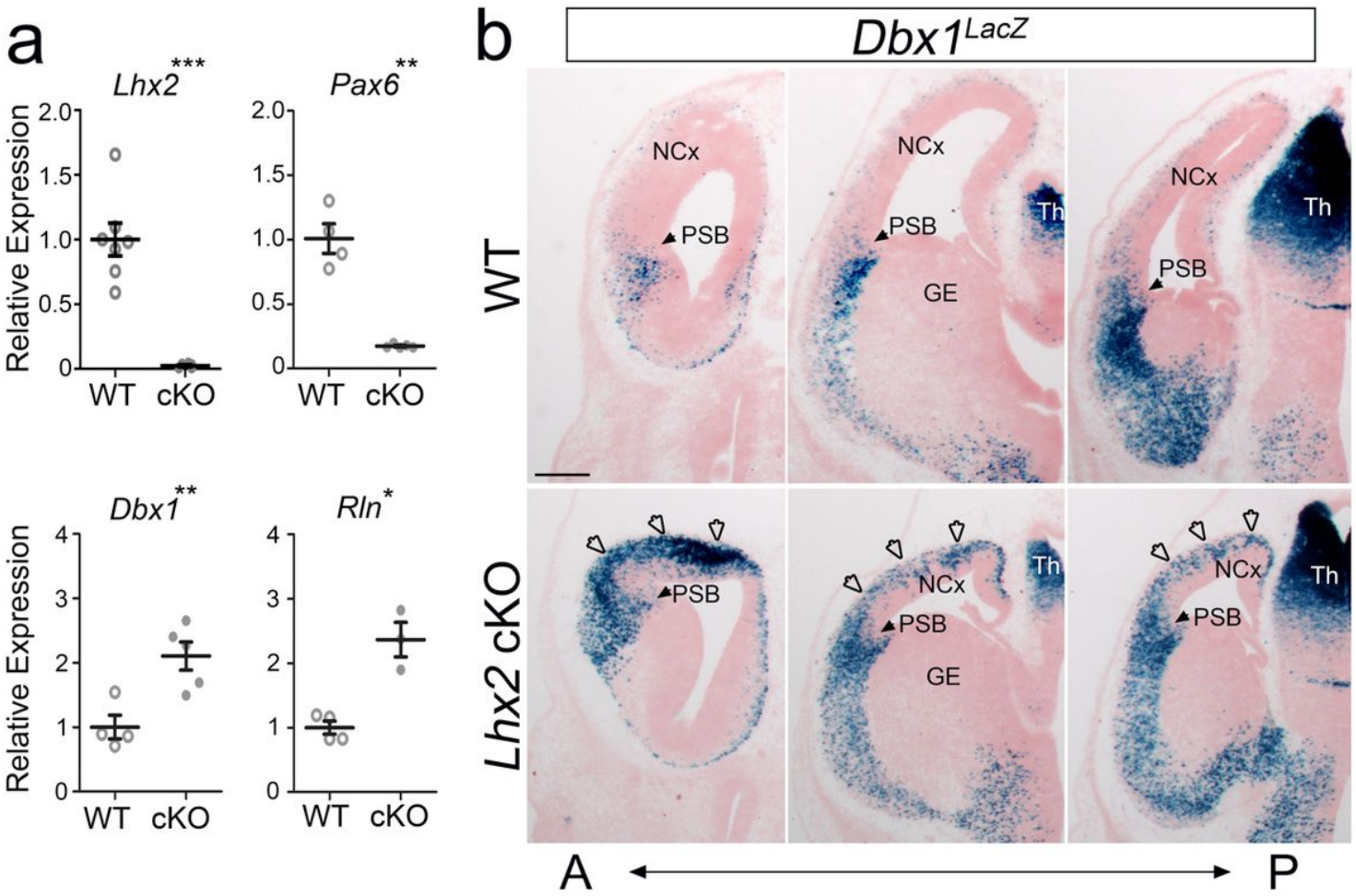

Figure 1

Dbx1 is upregulated in Lhx2 conditional knockout cortices. (a) Demonstrated by qPCR, the expression levels of Lhx2 and Pax6 are significantly downregulated in the cKO (Lhx2f/f; Emx1Cre) cortex when compared with WT (Lhx2fl/+) at E13.5, while the levels of Dbx1 and Rln are significantly upregulated in the cKO mice (n = 3-5; Lhx2, $P < 0.001$; Pax6, $P = 0.0054$; Dbx1, $P = 0.0085$; Rln, $P = 0.0412$). (b) LacZ staining on coronal sections of Dbx1LacZ cortices of WT (top) and cKO (bottom) embryos at E13.5. From anterior (A) to posterior (P), LacZ+ cells (blue) are specifically located in the pallial-subpallial boundary (PSB, arrowheads) in WT. An increased number of LacZ+ cells (indicated by unfilled arrowheads) was observed in the neocortex (NCx) of the cKO. Scale bar, 200 μm. GE, ganglionic eminence.

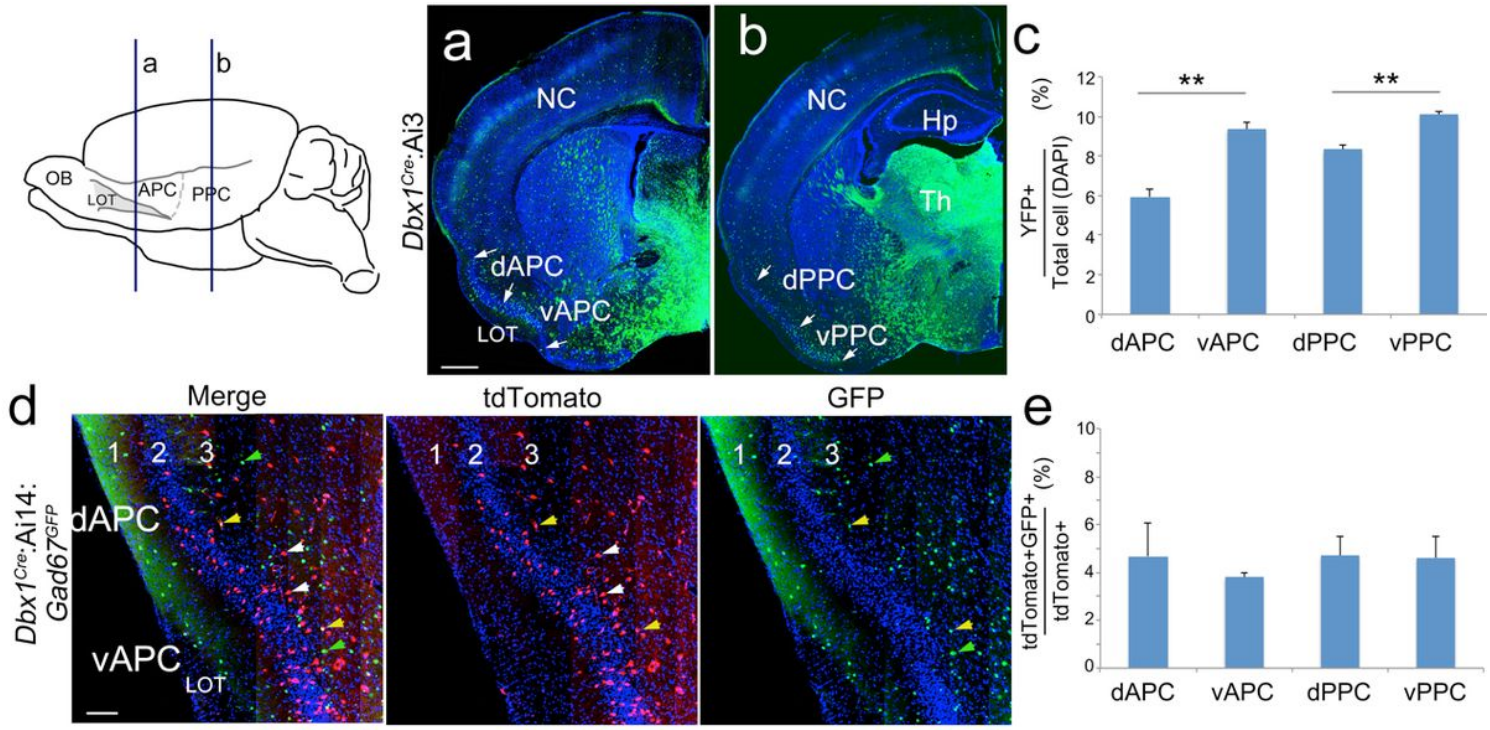

Figure 2

The contribution of cells of the Dbx1 lineage in piriform cortex. (a, b) Coronal sections of Dbx1Cre:Ai3 cortex at P7. Cells of the Dbx1 lineage were labeled by YFP and are shown at the level of the anterior piriform cortex (APC) and posterior PC (PPC), as indicated on the left. The APC and PPC are further divided into dorsal and ventral subregions. (c) Density of cells of the Dbx1 lineage (number of YFP+ cells/number of total cells) measured in a radial column in PC subregions. Dbx1 cell denisty is significantly higher in ventral PC regions. (d) Coronal sections at the level of the APC from Dbx1Cre:Ai14:Gad67GFP cortex at P30. Cells of Dbx1 lineage were labeled by tdTomato and inhibitory interneurons were labeled by GFP. GFP- and tdTomato-positive cells are indicated by green and white arrowheads respectively, while double-labeled cells are indicated by yellow arrowheads. (e) Quantification of the percentage of interneurons in the Dbx1 lineage (number of GFP+tdTomato+ cells/number of tdTomato+ cells). About 4% of the Dbx1 lineage cells are inhibitory interneurons, across the PC. LOT, lateral olfactory tract; OB, olfactory bulb; NC, neocortex; Hp, hippocampus. Scale bars, 500μm (a) and 100μm (d).

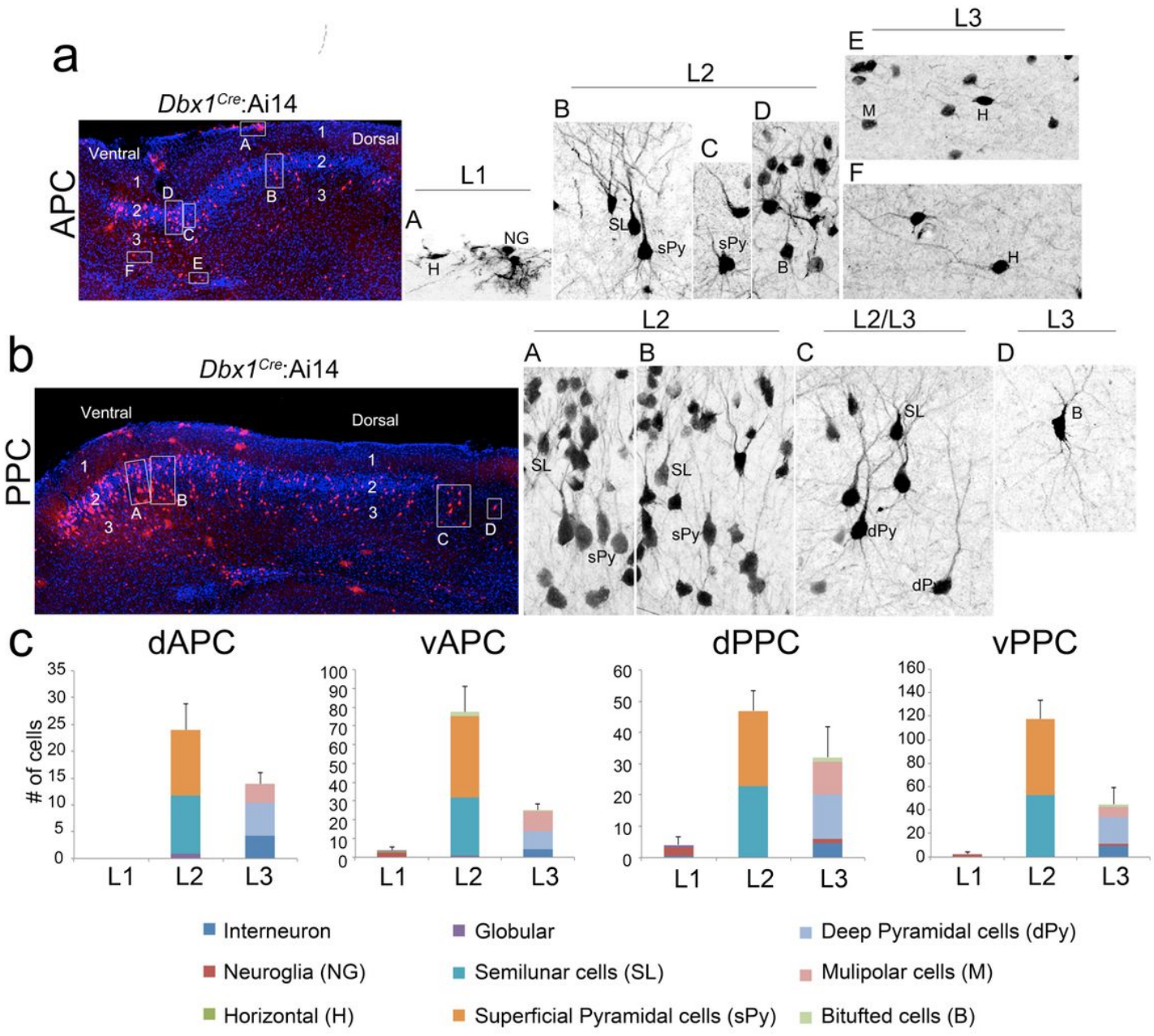

Figure 3

Morphology of neurons of the Dbx1 lineage. (a, b) Morphology of neurons of the Dbx1 lineage was observed in coronal sections of Dbx1Cre:Ai14 cortices at P30 at the levels of APC (a) and PPC (b) Images of insets are shown on the right at higher magnification. Different cell types, as indicated, were identified based on their morphology. (c) Quantification of the percentage of each cell type observed in different sub-regions across PC. Scale bar, 100μm.

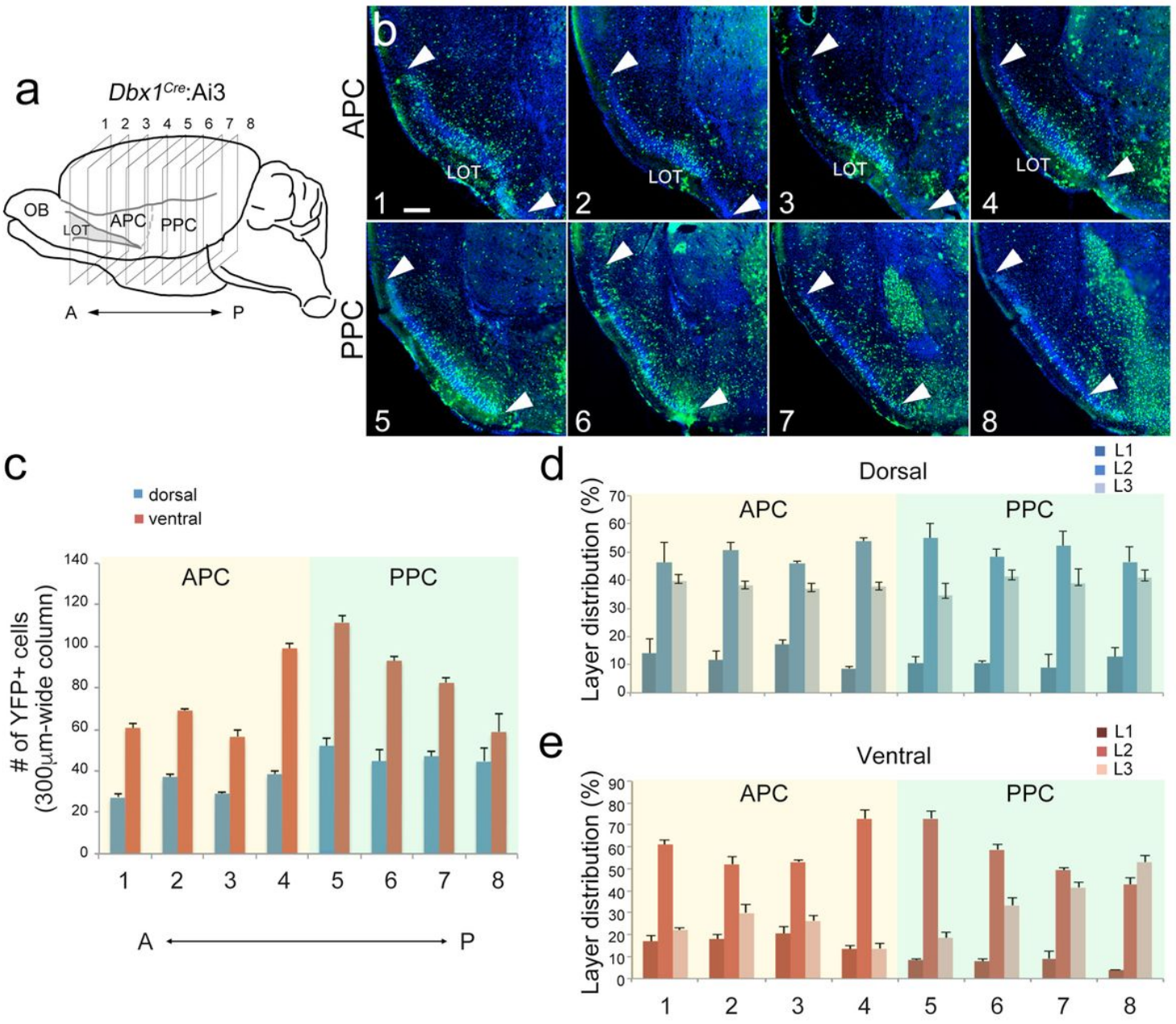

Figure 4

Neurons of the Dbx1 lineage show preference to distribute in ventral PC and in layer 2. (a, b) Coronal sections of Dbx1Cre:Ai3 cortex at P7 at eight levels from anterior (A) to posterior (P). (c) Quantification of the number of YFPexpressing cells in dorsal and ventral PC at each level. Higher numbers of YFP+ cells were found in the ventral PC compared to dorsal PC. (d, e) Quantification of laminar distribution of YFP+ cells. Most YFP+ cells were detected in layer 2 (L2), across the PC. Scale bar, 100μm.

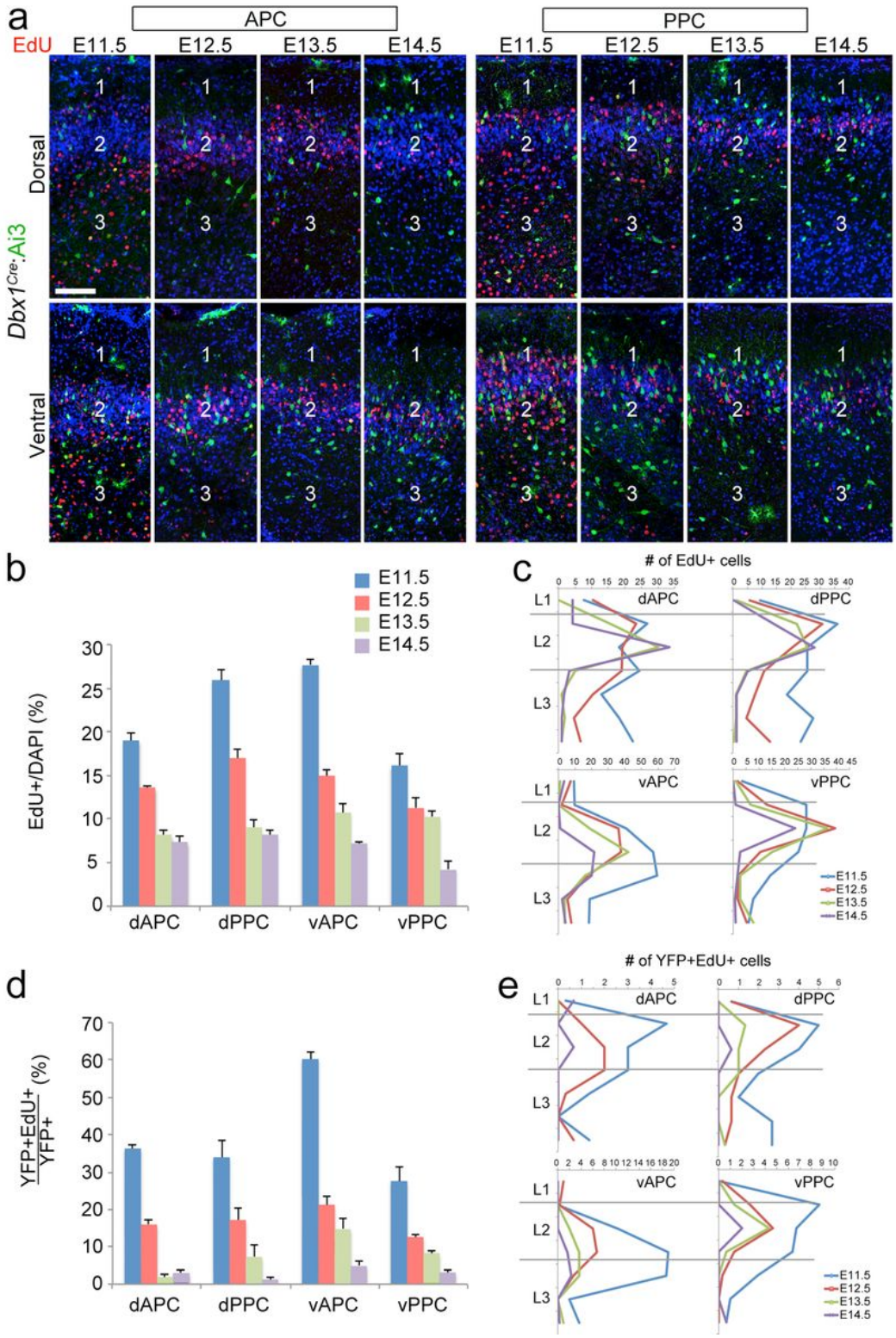

Figure 5

Neurons of the Dbx1 lineage are early born neurons in PC. (a) YFP (cells of the Dbx1 lineage, green) and EdU staining (red) in coronal sections from P7 Dbx1Cre:Ai3 mice. EdU was injected into pregnant mothers at indicated stages. (b-e) Quantification of results from (a), indicating the numbers and distributions of EdU+ cells (b, c) and EdU+YFP+ cells (d, e) at the indicated stages (n = 3). Scale bar, 100μm.

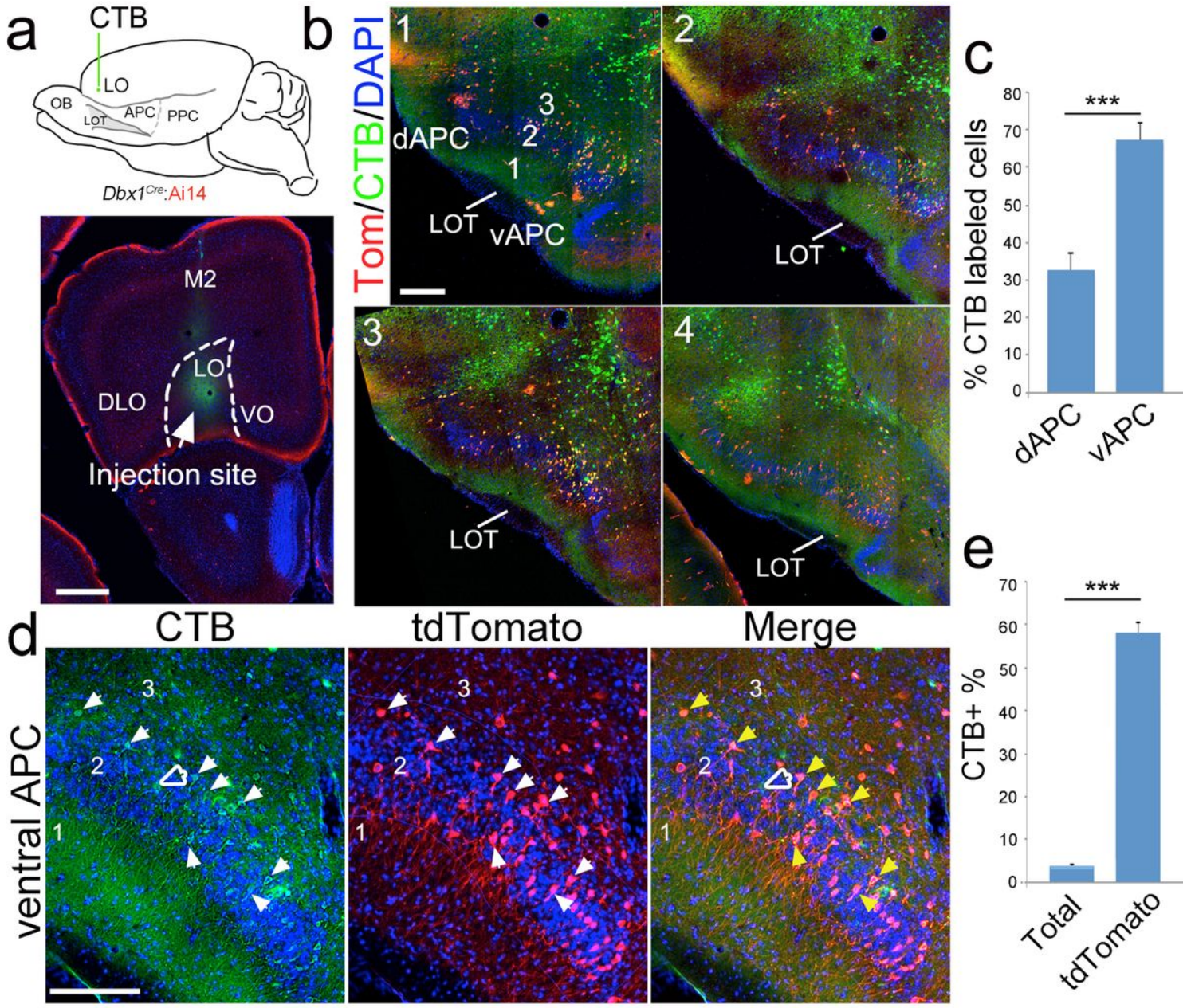

Figure 6

Neurons of the Dbx1 lineage in the ventral APC preferentially project to orbitofrontal cortex. (a) Green fluorescence (Alexa Fluor 488)- conjugated CTB was injected into the lateral orbitofrontal cortex (LO) in Dbx1Cre:Ai14 mice at P30. An injection site is shown in the coronal section (below). (b) CTB-labeled neurons (green) were detected throughout the APC (sections 1-4 from anterior to posterior). Neurons of the Dbx1 lineage were labeled by tdTomato (Tom+, red). (c) Significantly more CTB-labeled neurons were detected in the ventral APC than in the dorsal APC. (d) LO-projecting neurons (green) were enriched in L2 of the ventral APC. Green-only neurons are indicated by hollow arrowheads and yellow neurons (positive for both green and red) are indicated by solid arrowheads. (e) Among the total population of neurons in vAPC L2 (labeled by DAPI), about 4% were LO projection neurons (labeled by CTB). Significantly higher percentage of LO-projecting neurons was found within the neuronal population of the Dbx1 lineage (more than 50%). Scale bar, 500μm (a), 100μm (b) and 50μm (d).

Supplementary Files

This is a list of supplementary files associated with this preprint. Click to download.

- Supplementaryinfo.pdf